

FINITE ELEMENT ANALYSIS OF MAGNETO-HYDRODYNAMIC (MHD) MIXED CONVECTION FLOW ON A TRIANGULAR CAVITY.

Aki Farhana¹, Mohammed Nasir Uddin², Mohammad Abdul Alim³

¹Lecturer, Department of Mathematics, Mileston College, Dhaka,

²Department of Mathematics, Bangladesh University of Business & Technology (BUBT), Dhaka,
Bangladesh

³Department of Mathematics, Bangladesh University of Engineering & Technology (BUET), Dhaka, Bangladesh.

ABSTRACT

In this paper, the effect of magneto-hydrodynamic (MHD) on mixed convection flow within triangular cavity has been numerically investigate. The bottom wall of the cavity considered as heated. Besides, the left and the inclined wall of the triangular cavity are assumed to be cool and adiabatic. The consequent mathematical model is governed by the coupled equations of mass, momentum and energy and solved by employing Galerkin weighted residual method of finite element formulation. The present numerical procedure adopted in this investigation yields consistent performance over a wide range of parameters Rayleigh number Ra (10^3 - 10^4), Prandtl number Pr (0.7 - 3) and Hartmann number Ha (5 - 50). The numerical results are presented in terms of stream functions, temperature profile and nussult numbers. It is observed that the Hartmann and Rayleigh number has significant effect on the both flow and thermal fields.

Keywords: MHD, Mixed Convection, Triangular Cavity, Finite Element Method And Galerkin Weighted Residual Method.

1. INTRODUCTION

Many mathematicians, versed engineers and researchers studied the problems of MHD mixed convection for different types of cavity. Amongst them, Oreper and Szekely [2] studied the effect of an externally imposed magnetic field on buoyancy driven flow in a rectangular cavity. They found that the presence of a magnetic field can suppress natural convection currents and that the strength of the magnetic field is one of the important factors in determining the quality of the crystal. Ozoe and Maruo [3] investigated magnetic and gravitational natural convection of melted silicon two-dimensional numerical computations for the rate of heat transfer. Rudraiah et al. [4] investigated the effect of surface tension on buoyancy driven flow of an electrically conducting fluid in a rectangular cavity in the presence of a vertical transverse magnetic field to see how this force damps hydrodynamic movements. At the same time, Rudraiah et al.[5] also studied the effect of a magnetic field on free convection in a rectangular enclosure. The problem of unsteady laminar combined forced and free convection flow and heat transfer of an electrically conducting and heat generating or absorbing fluid in a vertical liddriven cavity in the presence of a magnetic field was formulated by Chamkha [1].Recently, Rahman et al.[6] studied the effect of a heat conducting horizontal circular cylinder on MHD mixed convection in a lid-driven cavity along with Joule Heating. The author considered the cavity

consists of adiabatic horizontal walls and differentially heated vertical walls, but it also contains a heat conducting horizontal circular cylinder located somewhere inside the cavity. The results indicated that both the flow and thermal fields strongly depend on the size and locations of the inner cylinder, but the thermal conductivity of the cylinder has significant effect only on the thermal field. Rahman et al.[7] investigated the effect on magnetohydrodynamic (MHD) mixed convection around a heat conducting Horizontal circular cylinder placed at the center of a rectangular cavity along with joule heating. They observed that the streamlines, isotherms, average Nusselt number, average fluid temperature and dimensionless temperature at the cylinder center strongly depend on the Richardson number, Hartmann number and the cavity aspect ratio. Very recently, Rahman et al. [8] made numerical investigation on the effect of magneto hydrodynamic (MHD) mixed convection flow in a vertical lid driven square enclosure including a heat conducting horizontal circular cylinder with Joule heating. The author found that the Hartmann number, Reynolds number and Richardson number have strong influence on the streamlines and isotherms.

To the best of our knowledge in the light of the above literatures, it has been pointed out that no work has been paid on MHD mixed convection inside a triangular cavity yet.

2. PHYSICAL MODEL AND ASSUMPTIONS

The physical model considered here is shown in Fig.-1, along with the important geometric parameters. The heat transfer and the fluid flow in a two-dimensional triangular cavity with MHD flow whose left wall and bottom wall are subjected to cold T_c and hot T_h temperatures respectively while the inclined walls are kept adiabatic. The fluid was assumed with Prandtl number ($Pr = 0.71, 1.0, 7.0$) and Newtonian, and the fluid flow is considered to be laminar. The properties of the fluid were assumed to be constant.

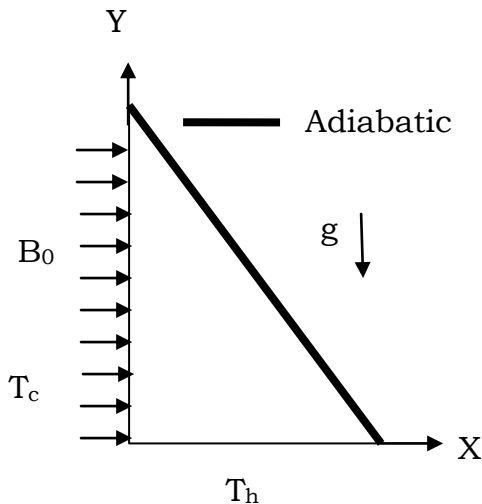


Fig1. Schematic diagram of the square open cavity

3. MATHEMATICAL MODEL

The fundamental laws used to solve the fluid flow and heat transfer problems are the conservation of mass (continuity equations), conservation of momentum (momentum equations), and conservation of energy (energy equations), which constitute a set of coupled, nonlinear, partial differential equations. For laminar incompressible thermal flow, the buoyancy force is included here as a body force in the v -momentum equation. The governing equations for the two-dimensional steady flow after invoking the Boussinesq approximation and neglecting radiation and viscous dissipation then the governing equations in non-dimensional form are written as follow:

$$\frac{\partial u}{\partial x} + \frac{\partial v}{\partial y} = 0 \dots \dots \dots (1)$$

$$U \frac{\partial U}{\partial X} + V \frac{\partial U}{\partial Y} = -\frac{\partial P}{\partial X} + \frac{1}{Re} \left(\frac{\partial^2 U}{\partial X^2} + \frac{\partial^2 U}{\partial Y^2} \right) \dots (2)$$

$$U \frac{\partial U}{\partial X} + V \frac{\partial U}{\partial Y} = -\frac{\partial P}{\partial Y} + \frac{1}{Re} \left(\frac{\partial^2 V}{\partial X^2} + \frac{\partial^2 V}{\partial Y^2} \right) + Ra Pr \theta - \frac{Ha^2}{Re} V \dots (3)$$

$$U \frac{\partial \theta}{\partial X} + V \frac{\partial \theta}{\partial Y} = \frac{1}{Re Pr} \left(\frac{\partial^2 \theta}{\partial X^2} + \frac{\partial^2 \theta}{\partial Y^2} \right) \dots (4)$$

With the boundary conditions
The dimensionless boundary conditions under consideration can be written as:

At the left vertical wall: $\theta = 0$

At the bottom wall: $\theta = 1$

$$\text{At the inclined wall: } \frac{\partial \theta}{\partial N} = 0$$

Where N is the non-dimensional distances either along X or Y direction acting normal to the surface and K is the dimensionless thermal conductivity. According to Singh and Sharif (2003), the average Nusselt number at the heated wall of the cavity based on the non-dimensional variables may be expressed as

$$Nu = - \int_0^{L_h/L} \frac{\partial \theta}{\partial X} dY \text{ and the bulk average}$$

temperature defined as $\theta_{av} = \int \theta d\bar{V} / \bar{V}$, where \bar{V} is the cavity volume.

The above equations were normalized using the following dimensionless scales:

$$X = \frac{x}{L} \quad Y = \frac{y}{L} \quad \mathbf{U} = \frac{\mathbf{u}}{U_0} \quad \mathbf{V} = \frac{\mathbf{v}}{U_0} \quad Pr = \frac{\nu}{\alpha}$$

$$Re = \frac{u_i L}{\nu}, Pr = \frac{\nu}{\alpha}, Gr = \frac{\beta g \Delta T L^3}{\nu^2}, Ha^2 = \frac{\sigma B_0^2 L^2}{\mu}, Ra = Gr \times Pr$$

$$\Delta T = T_h - T_c \text{ and } \alpha = \frac{\kappa}{\rho C_p}$$

4. NUMERICAL ANALYSIS

The governing equations along with the boundary conditions are solved numerically by employing Galerkin weighted residual finite techniques. The finite element formulation and computational procedure are omitted herein for brevity.

5. RESULTS AND DISCUSSION

The MHD mixed convection flow and temperature fields as well as heat transfer rates and bulk temperature inside the triangular cavity has been numerically investigated. The MHD mixed convection phenomenon inside the enclosure is strongly influenced by governing as well as physical parameters, namely and Hartman number Ha , Reynolds number Re , Prandtl number Pr , Rayleigh number Ra . As the nature of flow and thermo physical properties of fluid strongly influenced on the heat transfer rate, and the numerical computation were performed for a range of Ha , Re and Pr ($Ha=0.0-50$, $Re= 40-100$, $Pr=0.71-6$). In addition, for each value of mentioned parameters, computations are performed at $Ra = 5 \times 10^3$ that focuses on pure mixed convection. Moreover, the results of this study are presented in terms of streamlines and isotherms. Furthermore, the heat transfer effectiveness of the enclosure is displayed in terms of average Nusselt number Nu and the dimensionless average bulk temperature.

Obviously for high values of Ra number the errors encountered are appreciable and hence it is necessary to perform some grid size testing in order to establish a suitable grid size. Grid independent solution is ensured by comparing the results of different grid meshes for

$Ra = 10^5$, which was the highest Grashof number. The total domain is discretized into 41520 elements that results in 62280 nodes. In order to validate the numerical code, pure natural convection with $Pr = 0.71$ in a square open cavity was solved and the average Nusselt numbers is presented by graphically. The results were compared with those reported by Basak et al., obtained with an extended computational domain. In Table1, a comparison between the average Nusselt numbers is presented. The results from the present experiment are almost same as Basak et.al.

Table 1: Comparison of the results for the constant surface temperature with $Pr = 0.71$.

| Ra | Nu_{av} | |
|--------|--------------|---------------------|
| | Present work | Basak et al. (2007) |
| 10^3 | 5.49 | 5.40 |
| 10^4 | 5.77 | 5.56 |
| 10^5 | 7.08 | 7.54 |

5.1 Effects of Reynolds Number (Re)

The effects of Reynolds number on the flow structure and temperature distribution are depicted in Fig. 2.7. The streamlines are presented for different values of Rayleigh numbers (Ra), Reynolds numbers (Re) ranging from 10^3 to 10^4 and 40 to 100 respectively while $Pr = 0.71$, and $Ha=20$. Now at $Re = 40$, the fluid near to the hot (bottom) wall has lower density, so it moves upward while the relatively heavy fluid near to cold (left) wall and this fluid is heated up. Thus the fluid motion completes the circulation. Using the definition of stream function, the streamlines with $+\psi$ correspond to anti-clockwise circulation, and those with $-\psi$ correspond to clockwise circulation. A very small magnitude value of contour rotating cell is observed in the middle part of the cavity as primary vortex. The secondary vortex cell are shown around the primary vortex in the cavity. The secondary vortex are more packed to the respective wall dramatically for the increasing value of Re that's imply the flow moves faster and the velocity boundary layer become thinner. Moreover, it is clearly seen that the center vortex become bigger with increasing Re due to conduction intensified gradually. The value of the magnitudes of the stream function greater due to mechanically driven circulations.

The corresponding isotherm pattern for different value of Reynolds number while $Pr = 0.71$ and $Ha=20$ is shown in the Fig. 2. From this figure, it is found that the isotherms are more congested at the heated wall of the cavity testifying of the noticeable increase in convective heat exchange. The temperature gradients are very small due to mechanically driven circulations at the left wall of the cavity. It is also noticed that the thermal boundary layer near the heated wall becomes thinner with increasing Re . Due to high circulations, the temperature contours condensed in a very small

regime at the upper portion of the left wall and this may cause greater heat transfer rates at the heated wall. The effects of Reynolds number on average Nusselt number Nu at the heated wall and the average bulk temperature θ_{av} of the fluid in the cavity are illustrated in Fig 4 &5, while $Pr = 0.71$, $Ha=20$. From Fig.4(i), it is seen that the average Nusselt number Nu increases steadily with increasing Rayleigh number. This arises from the fact that physical properties of fluid changes to better heat transfer. For $Re = 100$, it is noticed that the average Nusselt number Nu increases sharply but for lower values of $Re (= 40)$ then the increase of Nu befall slower.

Fig. 5 displays the variation of the average bulk temperature against the Rayleigh number for various Reynolds numbers. The average temperature decreases smoothly with increase of Ra . It is an interesting observation that at lower Re , the average bulk temperature is affected by Rayleigh number.

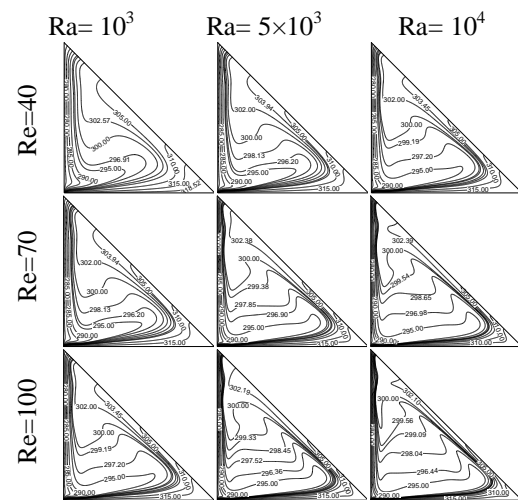


Fig 2: Isotherms patterns for different Re (40,70,100) when $Pr = 0.71$ and $Ha=20$

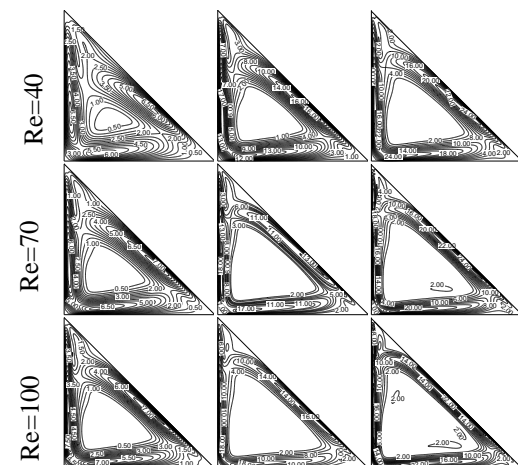


Fig 3: Streamlines patterns for different Re (20,70,100) when $P = 0.71$ and $Ha=20$

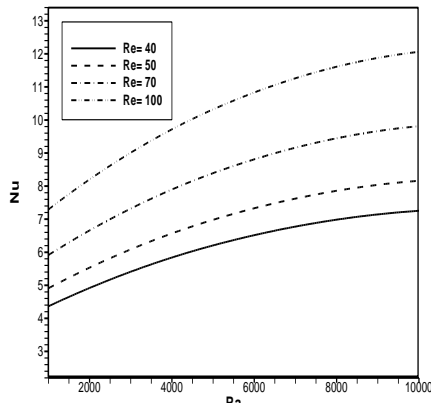


Fig-4: Effect of average Nusselt number and Rayleigh number while $Pr = 0.71$, $Ha = 20$.

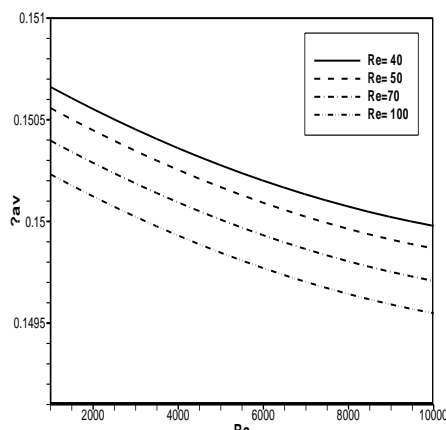


Fig.-5: Effect of average bulk temperature and Rayleigh number while $Pr = 0.71$, $Ha = 20$.

5.2 Effect of Prandtl Number (Pr)

The effects of Prandtl number on flow fields for the considered Ra is depicted in Fig.6&7, while $Re = 50$ and $Ha=20$ are kept fixed. Now, from the figure, it is seen that a small vortex is formed at the center of the cavity. It is evident that the size of the vortex is increased with the increasing value of Pr . The influence of Prandtl number Pr on thermal fields for the selected value of Ra is displayed in Fig.6 for $Re = 50$ and $Ha=20$. As expected, the thermal boundary layer decreases in thickness as Pr increases. This is reflected by the denser deserting of isotherms close to the heated wall and cooled wall as Pr increases. The spread of isotherms at low values of Pr is due to a strong stream wise conduction that decreases the stream wise temperature gradient in the field. At the increase of Pr the isotherms become linear in the cavity and impenetrable to respective wall. From the Fig. 6, it can easily be seen that the isotherms for different values of Pr at $Ra = 10^4$ are clustered near the heated horizontal wall and cooled vertical heated surface of the enclosure, indicating steep temperature gradient along the vertical direction in this region. Besides, the thermal layer near the heated wall becomes thinner moderately with increasing Pr .

The effects of Prandtl number on average Nusselt number Nu at the heated surface and average bulk temperature θ_{av} in the cavity is illustrated in Fig. 8 & 9 with $Re = 50$ and $Ha=20$. From this figure, it is found that the average Nusselt number Nu goes up penetratingly with increasing Pr . It is to be highlighted that the highest heat transfer rate occurs for the highest values of $Pr (= 6)$. The average bulk temperature of the fluid in the cavity declines very mildly for higher values of $Pr (0.71- 6.0)$. But for the lower values of Pr , the average bulk temperature is linear. It is to be mentioned here that the highest average temperature is documented for the lower value of $Pr (=0.71)$ in the free convection dominated region.

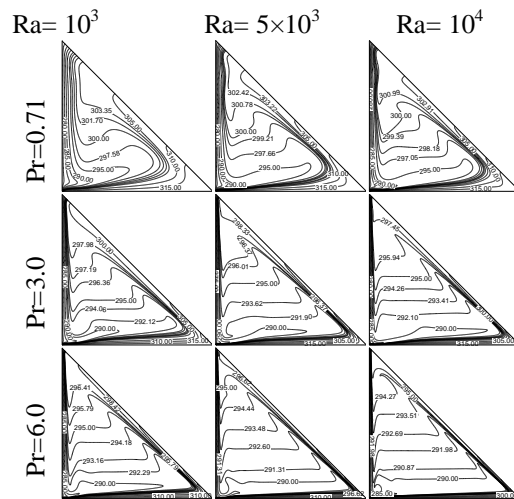


Fig-6: Isotherms patterns for different $Pr (0.71, 3.0, 6.0)$ when $Re = 50$ and $Ha=20$

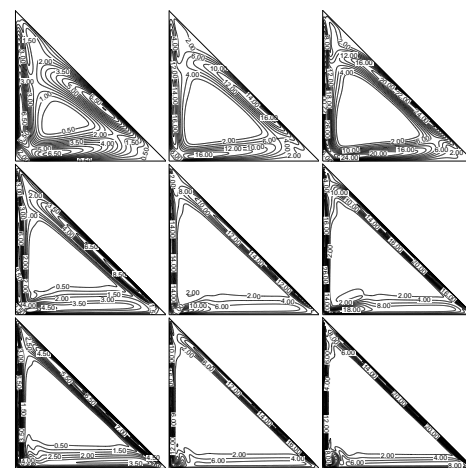


Fig-7: Streamline patterns for different $Pr (0.71, 3, 6)$ when $Re = 50$ and $Ha=20$

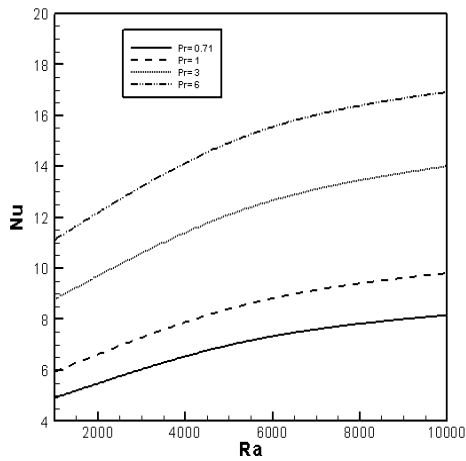


Fig 8: Effect of average Nusselt number and Rayleigh number while $Re = 50$ and $Ha=20$

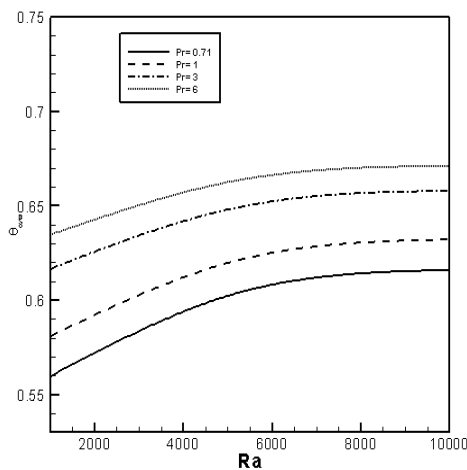


Fig 9: Effect of average bulk temperature and Rayleigh number while $Re = 50$ and $Ha=20$.

5.3 Effects of Hartmann Number

The influences of Hartmann number Ha on the flow and thermal fields at $Ra = 1e3$ to $1e4$ is illustrated in Figure 10 & 11, while $Pr = 0.71$ and $Re = 50$ are kept fixed. In absence of the magnetic field $Ha (= 0.0)$, a remarkable strong vortex is found near the center of the cavity. In this folder, the size of the counter clockwise vortex also decreases sharply with increasing Ha . This is because application of a transverse magnetic field has the tendency to slow down the movement of the buoyancy induced flow in the cavity. The effects of Hartmann number Ha on isotherms are shown in the Figure 10 while $Re = 50$ and $Pr = 0.71$ are kept fixed. In absences of magnetic field $Ha = 0.0$), it is observed that the higher values isotherms are more tightened at the vicinity of the heated wall of the cavity for the considered value of Ra . A similar trend is found for the higher values of Ha . From this figure it can easily be seen that isotherms are almost parallel at the vicinity of the bottom horizontal hot wall but it changes to parabolic shape with the increasing distance from inclined wall for the highest value of $Ha (=20.0)$ at $Pr=0.71$, indicating that most of the heat transfer process is carried out by conduction. In addition, it is noticed that

the isothermal layer near the heated surface becomes slightly thin with the decreasing Ha . However in the remaining area near the left wall of the cavity, the temperature gradients are small in order to mechanically driven circulations. The effects of Ha on average Nusselt number Nu at the heated surface and average bulk temperature θ_{av} in the cavity is illustrated in Fig. 12 & 13 with $Re = 50$ and $Pr = 0.71$. From this figure, it is found that the average Nusselt number Nu decreases with increasing Pr . It is to be highlighted that the highest heat transfer rate occurs for the lowest values of $Ha (= 5)$. The average bulk temperature of the fluid in the cavity is high for higher values of Ha ($0 - 6.0$). It is to be mentioned here that the highest average temperature is documented for the higher value of Ha in the free convection dominated region.

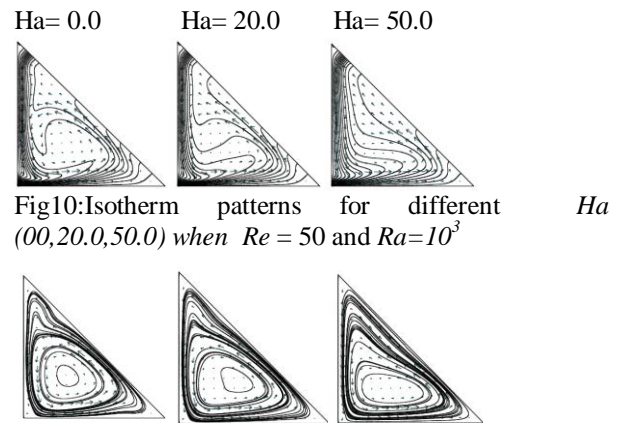


Fig10: Isotherm patterns for different Ha ($00,20.0,50.0$) when $Re = 50$ and $Ra=10^3$

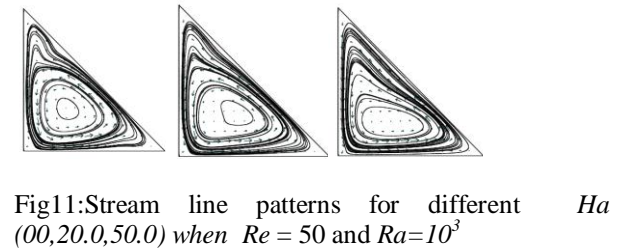


Fig11: Stream line patterns for different Ha ($00,20.0,50.0$) when $Re = 50$ and $Ra=10^3$

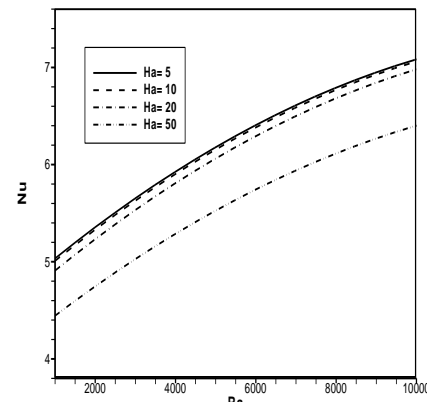


Fig 12: Effect of average Nusselt number and Rayleigh number while $Pr = 0.71$ and $Re = 50$.

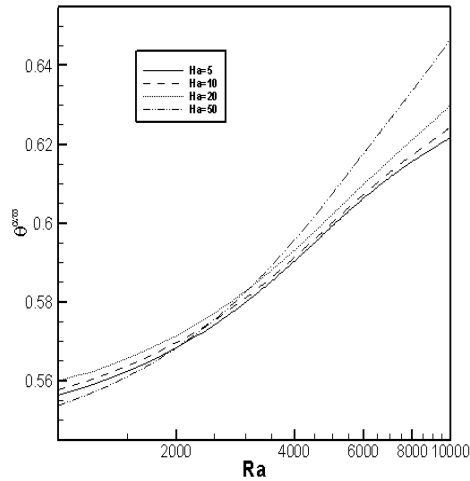


Fig.13: Effect of average bulk temperature and Rayleigh number while $Pr = 0.71$ and $Re = 50$

7. CONCLUSION

A finite element method for steady-state incompressible conjugate effect of mixed convection and conduction has been presented. The finite element equations were derived from the governing flow equations that consist of the conservation of mass, momentum, and energy equations. The derived finite element equations are nonlinear requiring an iterative technique solver. The Galerkin weighted residual method is applied to solve these nonlinear equations for solutions of the nodal velocity components, temperatures, and pressures. The above example demonstrates the capability of the finite element formulation that can provide insight to steady-state incompressible conjugate effect of mixed convection and conduction problem.

8. NOMENCLATURE

| Symbol | Meaning | Unit |
|--------|-----------------------------------|-------------------|
| g | gravitational acceleration | (ms^{-2}) |
| Gr | Grashof number | |
| Ha | Hartmann Number | |
| Re | Reynolds Number | |
| Ra | Rayleigh Number | |
| k | thermal conductivity of the fluid | $(Wm^{-1}K^{-1})$ |
| L | height and width of the enclosure | (m) |

| | | |
|----------|---------------------------------------|---------------|
| Nu | Nusselt number | |
| P | pressure | (Nm^{-2}) |
| Pr | Prandtl number, ν/α | |
| q | heat flux | (Wm^{-2}) |
| T | temperature | (K) |
| x, y | Cartesian coordinates | (m) |
| X, Y | non-dimensional Cartesian coordinates | |
| θ | dimensional temperature | |
| u, v | velocity components | (ms^{-1}) |
| α | thermal diffusivity | (m^2s^{-1}) |
| β | thermal expansion coefficient | (K^{-1}) |
| ρ | density of the fluid | (kgm^{-3}) |
| ν | kinematic viscosity of the fluid | (m^2s^{-1}) |

9. REFERENCES

- [1] Chamkha, A. J., "Hydromagnetic combined convection flow in a vertical lid-driven cavity with internal heat generation or absorption", Numer. Heat Transfer, Part A, Vol. 41, pp. 529-546, 2002.
- [2] Oreper, G. M., Szekely, J., "The effect of an externally imposed magnetic field on buoyancy driven flow in a rectangular cavity", J. of Crystal Growth, Vol. 64, pp. 505-515, 1983.
- [3] Ozoe, H., and Maruo, M., "Magnetic and gravitational natural convection of melted silicon-two dimensional numerical computations for the rate of heat transfer", JSME, Vol. 30, pp. 774-784, 1987.
- [4] Rudraiah, N., Venkatachalappa, M., and Subbaraya, C. K., "Combined surface tension and buoyancy-driven convection in a rectangular open cavity in the presence of magnetic field", Int. J. Non-linear

- Mech., Vol. 30(5), pp. 759-770, 1995a.
- [5] Rudraiah, N., Barron, R. M., Venkatachalappa, M., and Subbaraya, C. K., "Effect of magnetic field on free convection in a rectangular enclosure", *Int. J. Engng. Sci.*, Vol. 33, pp. 1075-1084, 1995b.
- [6] Rahman, M.M., Mamun M.A.H., Saidur, R., and Nagata Shuichi, "Effect Of a Heat Conducting Horizontal Circular Cylinder on MHD Mixed Convection In A Lid- Driven Cavity Along With Joule Heating", *Int. J. of Mechanical and Materials Eng. (IJMME)*, Vol. 4, No. 3, pp.256-265, 2009a.
- [7] Rahman, M. M., Alim, M. A., Chowdhury, M. K., "Magnetohydrodynamic mixed convection around a heat conducting horizontal circular cylinder in a rectangular lid-driven cavity with Joule heating", *J. Sci Res. I* (3), pp.461-472, 2009b
- [8] Rahman, M. M., Alim, M. A., "MHD mixed convection flow in a vertical lid-driven square enclosure including a heat conducting horizontal circular cylinder with Joule heating", *Nonlinear Analysis: Modeling and Control*, Vol 15, No. 2, pp.199-211, 2010.

9.MAILING ADDRESS

Mohammad Abdul Alim

Department of Mathematics, Bangladesh University of Engineering & Technology (BUET), Dhaka, Bangladesh.

Email: akibuet@gmail.com